Earthquake Engineering, Tenth World Conference © 1992 Balkema, Rotterdam. ISBN 90 5410 060 5

The dynamic constitutive model of loess under irregular seismic loading

Wang Lanmin, Zhang Zhenzhong & Wang Jun
Seismological Institute of Lanzhou, SSB, People's Republic of China

ABSTRACT: The loess is a sort of weak cohesion soil with porous microstructure formed in Quaternary. It is distributed widely in Northwestern China, and all of the historical earthquakes in the loess region have induced serious disasters. In this paper, it was verified that the dynamic constitutive relationship of undisturbed unsaturated loess under irregular seismic loading also obeys a hyperbolic model by means of a dynamic triaxial test system. But parameters of the model are different with different time histories of irregular seismic loading. The contrasting research was made in parameters, shear modulus and damping ratio under irregular seismic loading and equivalent sinusoidal loading. The quantitative relationship between the parameters of the model and predominant period of the applied irregular seismic load was initially established. Based on data of tests and calculations, it was confirmed that the Mansing Law is suitable for loess.

1 INTRODUCTION

The research on the dynamic constitutive model of loess and its parameters may provide the indexes of dynamic property for dynamic response analysis of loess deposit. It is one of the key links of seismic response analyses and calculations of building ground, natural slope and geotextile, affecting directly the reliability of the results. The results of dynamic triaxial tests given by Zhihui and Dingyi (1986) and Ruwen et al (1990) show that the dynamic constitutive relationship of loess under sinusoidal cyclic loading obeyed a hyperbolic model. However, the data on the dynamic properties of loess under irregular seismic loading are lacking in the world.

It is known that seismic loading is a kind of dynamic loading whose amplitude and frequency are irregular variable. Therefore, it is only an approximate and simplified way to research the dynamic properties of loess under the effect of earthquakes using regular loading of single frequency instead of irregular seismic loading. The authors performed the experimental research on the dynamic properties of loess under irregular seismic loading by means of a dynamic triaxial test system which can apply an axial load of arbitrary waveform on soil samples. In this paper, these results were summed up and discussed.

2 SEISMIC LOADS AND LOESS SAMPLES USED IN THE TESTS

The parameters and patterns of three irregular seismic loads used in the present tests are shown in Table 1, Fig.1(a), Fig.2(a) and Fig.3(a).

Table 1. The parameters of irregular seismic loads used in the tests

Load number	1	2	3
Predominant period(s)	0.17	0.42	1.00
Duration(s)	11.0	18.5	4.0
Load type	cycle	shock	cycle
Simulating seismic intensity	8	7	--

where No.1 is the artificial seismic wave from the analysis result of seismic risk in Lanzhou, No.2 is a UD-component of a strong aftershock (Ms=6.7) accelerogram on the ground surface of loessial deposits with the thickness of 4 meters during the Wuqia Ms 7.4 earthquake in Xinjiang Uygur Autonomous Region in 1985, No.3 is an irregular sample wave which is specially made for examining

the suitability of the general Mansing's Law for intact loess so as to compare clearly the calculated hysteresis curve with the tested one.

Loess samples used in the tests were secured from the depth of 5 meters in Pengjiaping village of Lanzhou. They are typical undisturbed unsaturated ones of Malan loess (Q_3) which is subject to failure under the effect of earthquakes. Their natural unit weight and water content are respectively 14.84 KN/m^3 and 9.7 percent. Before the tests, all of the loess samples were cut to lumps with diameter of 5 cm and length of 10 cm.

3 TEST PERFORMANCE

In the tests, a scheme of gradually applying load in the range of elastic strain of specimens was adopted. First, a specimen was consolidated under the virgin overburden pressure with a consolidation ratio, i.e. reciprocal of lateral pressure coefficient K_o, simulating the static stress state in which the specimen was in original deposits. After the consolidation deformation became stable, the irregular stress change of seismic loading time history was transferred to a specimen by the up-and-down movement of the triaxial loading piston. The time histories were repeatedly applied on the specimen a sequence after a sequence until the obvious residual strain developed in the specimen. For each sequence, the amplitude of the time history was properly raised. In the meantime, the time change curves of irregular stress and strain and the hysteresis loop in the course of each loading sequence were recorded respectively by a multi-channel oscillographic strip recorder and a X-Y function plotter. The time histories of the recorded axial strains respectively corresponding to the three loadings were shown in Fig.1, Fig.2 and Fig.3.

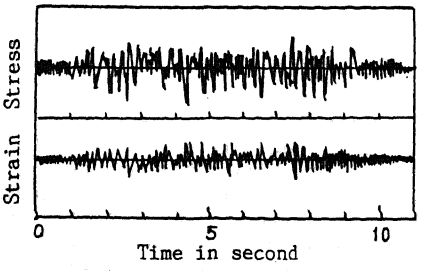

Fig.1 A group of recorded time histories of stress and strain in the test of No.1 irregular load.

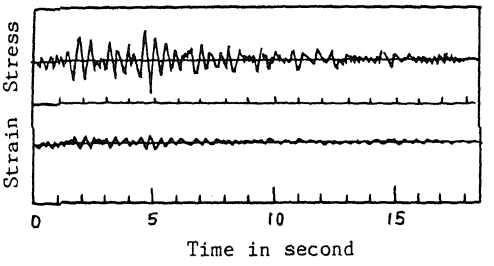

Fig.2 A group of recorded time histories of stress and strain in the test of No.2 irregular load.

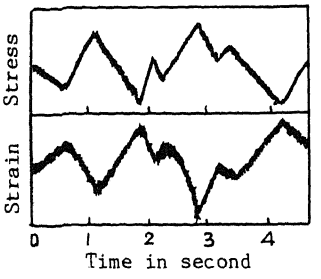

Fig.3 A group of recorded time histories of stress and strain in the test of No.3 irregular load.

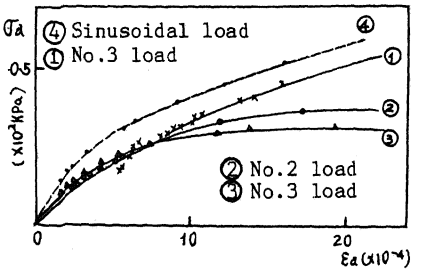

Fig.4 The stress-strain relationship curves under the four loadings.

4 THE DYNAMIC CONSTITUTIVE MODEL

The maximum amplitude of each recorded axial dynamic stress sequence, σ_d, was plotted against the axial dynamic strain corresponding to it. After the points (ε_d, σ_d) were connected by using a smooth curve, the plots of σ_d against ε_d as shown in Fig.5 would be gained. When the curves in Fig.5 was changed into the curves of ε_d/σ_d-ε_d in Fig.6, we found that these curves are approximately a group of straight lines. The equation of the straight lines is

$$\frac{\varepsilon_d}{\sigma_d} = a + b\varepsilon_d \qquad (1)$$

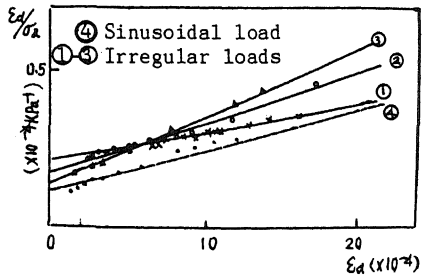

Fig.5 The relationships of ε_d/σ_d-ε_d under the four loadings.

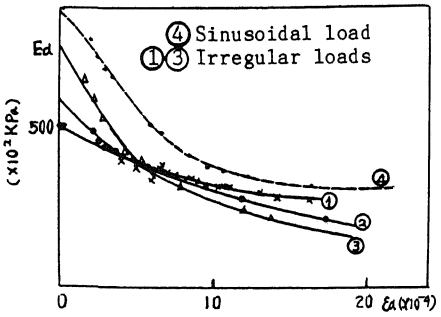

Fig.6 The relationships of E_d- ε_d under the four loadings.

or

$$\sigma_d = \frac{\varepsilon_d}{a+b\varepsilon_d} \tag{2}$$

where a and b are respectively the intercept on the axis of ε_d/σ_d and slope ratio of the straight line. It is known that equation (2) is the Hardin-Drnevich hyperbolic model. Consequently, the dynamic constitutive model of undisturbed unsaturated loess under irregular seismic loading may be described with a mathematical expression of hyperbola.

From the equation (1), we can obtain that

$$E_d = \frac{1}{a+b\varepsilon_d} \tag{3}$$

where E_d is dynamic elastic modulus. In equation (3), if ε_d is taken as zero, E_d may be written as

$$E_d = E_{dmax} = E_o = \frac{1}{a} \tag{4}$$

In equation (2), if ε_d tends to infinity, the limit of σ_d may be written as

$$\lim_{\varepsilon\to\infty} \sigma_d = \sigma_{dult} = \frac{1}{b} \tag{5}$$

If we order that

$$\frac{\sigma_{dult}}{E_{dmax}} = \varepsilon_r \tag{6}$$

ε_r may be written as

$$\varepsilon_r = \frac{a}{b} \tag{7}$$

To sum up, the physical means of a and b are that

$$a = \frac{1}{E_o}$$

$$b = \frac{1}{\sigma_{dult}} \tag{8}$$

$$\frac{a}{b} = \varepsilon_r$$

where E_o, σ_{dult} and ε_r are respectively initial elastic modulus, ultimate axial dynamic stress and reference axial dynamic strain as shown in Fig.7.

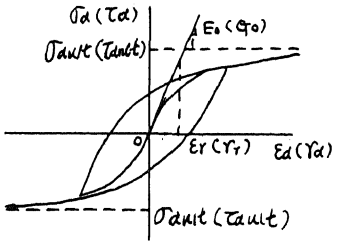

Fig.7 Hyperbolic model diagram.

According to the conversion relationships between axial dynamic stress, σ_d, and dynamic shear stress, τ_d, as well as between axial dynamic strain, ε_d, and dynamic shear strain, γ_d presented in formula (9), σ_d and ε_d recorded in dynamic triaxial test can be converted into

$$\tau_d = \frac{\sigma_d}{2}$$

$$\gamma_d = \varepsilon_d(1+\mu) \tag{9}$$

where μ is dynamic Poisson's ratio which is approximately taken as elastic Poisson's ratio. The relationship curve of τ_d-γ_d also obeys the same mathematical model as that of σ_d-ε_d, i.e

$$\tau_d = \frac{\gamma_d}{A+B\gamma_d} \tag{10}$$

as well as

$$A = \frac{1}{G_o}$$
$$B = \frac{1}{\tau_{dult}} \qquad (11)$$
$$\frac{A}{B} = \gamma_r$$

where G_o, τ_{dult} and γ_r are successively initial shear modulus, ultimate shear stress and reference shear strain. The parameters in parentheses of Fig.7 expressed their physical meanings. The quantitative relationships between a and A as well as b and B can be obtained from equation (2), (9) and (10), i.e

$$A = 2(1+\mu)a$$
$$B = 2b \qquad (12)$$

5 COMPARISON BETWEEN MODEL PARAMETERS UNDER IRREGULAR LOADING AND THOSE UDNER SINUSOIDAL LOADING

In order to compare the model parameters and the plots of modulus, E_d versus ε_d, of loess under irregular seismic loading with those under sinusoidal cyclic loading, dynamic triaxial tests under the two kinds of loading were performed using the same sort of loess sampels. The frequence of sinusoidal loading used in the tests is 1 H_z which is generally used in soil engineering tests. The test results have presented in Fig.4, Fig.5 and Fig.6. In the figures, the dashed lines indicate the results under sinusoidal loading and solid lines denote those under irregular seismic loadings.

It is easily seen from Fig.5 that all of the values of a under irregular seismic loading are greater than those under the sinusoidal loading equivalent to it and the values of b are different for different loading time histories. Fig.6 shows that in the same level of axial dynamic strain, the elastic modulus under irregular seismic loadings is always less than that under the sinusoidal loading equivalent to it. For Fig.5, the relevant errors in a and b under the above-mentioned two sorts of loadings range respectively from 20% to 90% and from 23% to 70%. For Fig.6, the range of relevant error in elastic modulus udner the two sorts of loadings is about 14-50%. These test results are sufficient for showing that there is a notable deviation between the dynamic parameters of loess under the irregular seismic loading and those under the sinusoidal equivalent seismic loading. For this reason, it is only an approximate and simplified method to perform the tests of dynamic properties of loess using sinusoidal load instead of irregular seismic load. The error caused by it can't be neglected. It is also shown that, for the same amplitude of stress, loess will develop greater deformation and fail easier when it is subjected to the effect of irregular seismic loadings.

6 THE EFFECT OF PREDOMINATE PERIOD ON THE MODEL PARAMETERS

The plots of γ_d/ε_d against γ_d and the plots of G_d against γ_d under the three irregular seismic loadings converted from the curves of ε_d/σ_d-ε_d and E_d-ε_d are respectively presented in Fig.8 and Fig.9. The curves of G_d/G_o-γ_d got by unitizing G_d with G_o in Fig.9 are shown in Fig.10. Fig.8 indicates that the value of A or B under an irregular

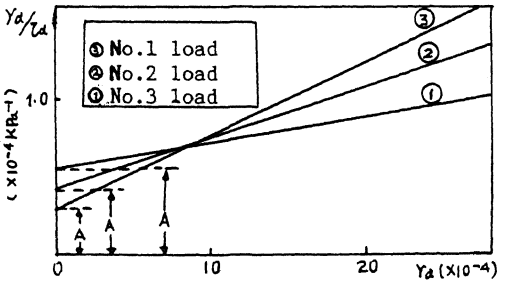

Fig.8 The relationships of γ_d/τ_d versus γ_d under different irregular loadings.

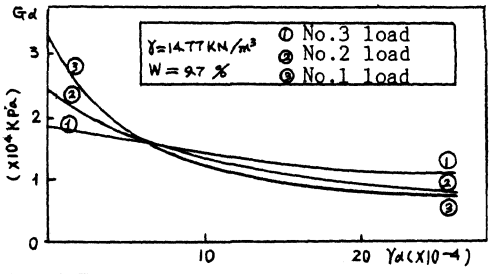

Fig.9 The relationships of G_d versus γ_d under different irregular loadings.

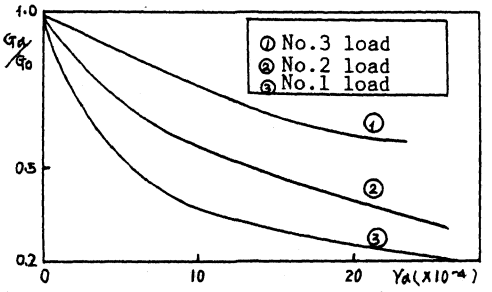

Fig.10 The relationships of G_d/G_o versus γ_d under different irregular loadings.

seismic load whose predominant period is longer is greater or less than the value of A or B under that whose predominant period is shorter. The authors found out initially the relationship between A or B and the predominant period, T_p, of an irregular seismic loading applied on loess sampels, as in formula (13)

$$A=(0.5795-0.2881T_p)\times10^{-4},\quad R=-0.9667$$
$$B=0.601+1.388T_p\ ,\qquad r=0.9592 \tag{13}$$

where r is a correlation coefficient, the units of A and T_p are respectively KPa^{-1} and second, and B is dimensionless.

Although only the test results of the three different irregular seismic loading are not enough to gain the final quantitative relationship between the parameters of loess dynamic constitutive model and the predominant period, moreover, the factors affecting the values of A and B maybe also involve the other key parameters of the time history of an irregular seismic loading, such as type, duration, and response spectrum of the seismic load, equation (8) shows at least that there is truly a very close correlation relationship between A or B and T_p. This implies that the predominant period, T_p, is probably one of key factors affecting the parameters of loess dynamic constitutive model, A and B.

In addition, Fig.7 shows that the shorter the predominate period is, the less the initial shear modulus is. The maximum relavant error among the three initial shear moduli is 78%. After γ_d is greater than or equal to 7×10^{-4}, the maximum relevant error in the dynamic shear modulus is about 24% at the same level of shear strain. It can be seen that the decaying rate of shear modulus with shear strain increasing is different for different time histories of irregular seismic loadings, and the longer the predominant period is, the greater the decaying rate is. But after γ_d is greater than or equal to 7×10^{-4}, the decaying rates of the three curves tend to be consistent. It is necessary to point out that the three curves in Fig.8 and Fig.9 intersect at a point and the reason why they do so remains to be researched further.

7 EXAMINATION INTO THE GENERAL MANSING'S LAW

In the present study, according to the general Mansing's Law, the hysteresis loops of shear stress, τ_d, and shear strain, γ_d, under an irregular seismic loading were calculated by two groups of parameters, A and B, one of which was gained from the test result with an irregular seismic loading and the other of which was gained from the test

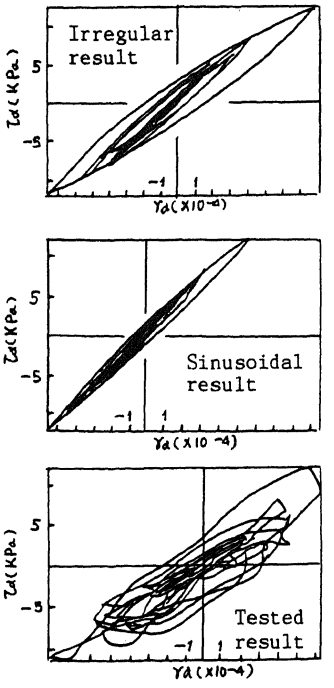

Fig.11 The hysteresis loops from calculation and test under No.2 irregular load.

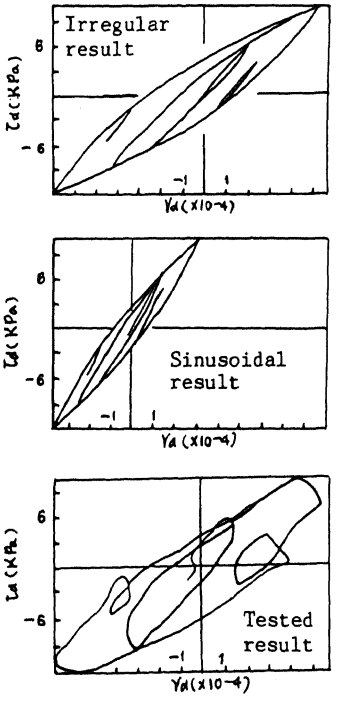

Fig.12 The hysteresis loops from calculation and test under No.3 irregular load.

result with its equivalent sinusoidal loading, to examine the suitability of the general Mansing's Law for loess. The calculated and tested hysteresis loops under the effects of the acceleration record wave of the strong earthquake and the irregular sample wave are respectively presented in Fig.11 and Fig.12. The two figures show that the sizes of hysteresis loops and their stress paths calculated by the model parameters, A and B, gained from the irregular loading test are basically identical with those recorded in the tests. By comparison, the hysteresis loops calculated by the model parameters gained from the equivalent sinusoidal loading tests are smaller than those recorded in the tests though their stress paths are similar to those recorded in the test. This result was also reported in the test result with random explosion wave given by Hengli and Zhenzhong (1988). Therefore, when the hysteresis loops of loess under the effect of earthquakes are calculated according to the Mansing's Law, the model parameters gained from the irregular seismic loading test should be used. If those results gained from the equivalent sinusoidal loading test are used in the calculation, the calculated results will need to be corrected. For the same reason, the time histories of dynamic shear strain calculated by the parameters given from the irregular seismic loading test are coincident with the test results and the amplitude of dynamic shear strain calculated by the parameters given from the equivalent sinusoidal loading test is less than the test result. But all of calculated time histories of dynamic shear strain are similar in shape to test time histories of dynamic shear strain.

8 CONCLUSION

The dynamic constitutive model of undisturbed unsaturated loess under irregular seismic loadings can be described by a hyperbolic mathematical expression which is the same as that under sinusoidal cyclic loadings. But the model parameters and shear modulus under the two kinds of loadings are different. Even for various time histories of irregular seismic loadings, these parameters are not same in value. Moreover, the relevant error caused by this kind of difference in some cases is too great to be ignored. Therefore, it will be necessary to use one or several time histories of irregular seismic loadings which are predicted to attack this loess site in the future to perform dynamic test of loess under the effect of earthquakes.

The dynamic property parameters of loess under the effect of earthquakes are closely related to the predominant period of an irregular seismic loading. The effect of the other factors of the seismic loading on dynamic properties of loess still needs to study further.

The general Manshing's Law is suitable to loess. If the hyperbolic model parameters from an irregular seismic loading test are used to calculate the time history of dynamic shear strain and the hysteresis loop, the calculated results need not to be corrected. If those parameters from an equivalent sinusoidal loading test are used, the calculated results need to be corrected.

REFERENCES

Henli, Z. & Zhenzhong, Z. 1988. Random exciting to loess sample on triaxial apparatus. Proc. ICEPRS: 348-351, Beijing.

Rewen, D., Zhenzhong, Z., Lan, L. & Juen, W. 1990. The further research in the dynamic properties of loess. Northwestern Seismological Journal, 12:72-78.

Zhihui, W. & Dingyi, X. 1986. The further approach on the dynamic properties of intact loess. Proc. National symposium on soil engineering buildings and ground antiearthquake, Xian: 219-224.